Multiple Model Adaptive Evasion Against a Homing Missile

Robert Fonod* and Tal Shima†

Technion - Israel Institute of Technology, 32000 Haifa, Israel

Multiple model adaptive evasion strategies from an incoming homing missile are presented. The problem is formulated in the context of an evading target aircraft having imperfect information on the relative state and on the employed guidance law and guidance parameters of the missile. The missile's guidance strategy is assumed to belong in a finite set of linear guidance laws and to be fixed throughout the engagement. Arbitrary-order linear missile and target dynamics, bounded target control, and nonlinear kinematics are also assumed. The filter used to identify the missile's guidance strategy is a nonlinear adaptation of the multiple model adaptive estimator, in which each model represents a possible guidance law and corresponding guidance parameters of the attacking missile. Specific limiting cases are carefully analyzed in which the attacking missile uses proportional navigation, augmented proportional navigation, or optimal guidance law. Matched optimal evasions from these specific cases are also derived and fit into the framework of the multiple model adaptive control approach. For the limiting cases, an alternative reduced-order approach is proposed to save computational resources. Considering noisy bearing-only measurements, the performance of the proposed evasion concepts is compared through a Monte Carlo simulation campaign to the scenario when the target has full knowledge about the attacking missile and the relative state.

Nomenclature

$[0]$	=	matrix of zeros with indicated dimension
$a_{(\cdot)}$	=	lateral acceleration, m/s^2
$a_{(\cdot)}^{max}$	=	maximal maneuvering capability, m/s^2
$\boldsymbol{A}$, $\boldsymbol{B}$, $\boldsymbol{C}$	=	state-space model of the linearized evasion problem
$\boldsymbol{A}_{(\cdot)}$, $\boldsymbol{B}_{(\cdot)}$, $\boldsymbol{C}_{(\cdot)}$, $d_{(\cdot)}$	=	state-space model of the entity's dynamics
$\boldsymbol{f}$	=	nonlinear equations of motion
$\boldsymbol{H}$	=	measurement matrix
$J_{(\cdot)}$	=	cost function
$k_{(\cdot)}$	=	parameter used for linearization
N'	=	navigation gain
p	=	number of possible regimes/filters
$\boldsymbol{P}$	=	state covariance matrix
r	=	range, m
$\boldsymbol{R}$	=	measurement covariance matrix
s_{MT}	=	switching function
$\boldsymbol{S}$	=	covariance matrix of the innovation sequence
t, t_{go}, t_f	=	time, time-to-go, and final time, respectively, s
T_s	=	sampling period

*Postdoctoral Fellow, Department of Aerospace Engineering, robert.fonod@technion.ac.il.

†Associate Professor, Department of Aerospace Engineering, tal.shima@technion.ac.il. Associate Fellow AIAA.

$V_{(\cdot)}$	=	speed, m/s
$\boldsymbol{v}$	=	measurement noise vector
$u_{(\cdot)}$	=	acceleration command, m/s^2
$\boldsymbol{x}$	=	state vector used for estimation
$\boldsymbol{y}$	=	state vector of the linearized evasion problem
$\boldsymbol{y}_{(\cdot)}$	=	entity's internal dynamics state vector
$\boldsymbol{z}_k$	=	measurement vector at time t_k
$\boldsymbol{z}_{1:k}$	=	measurement history up to time t_k
$X-O-Y$	=	Cartesian reference frame
Z	=	zero-effort miss, m
α	=	ratio between the weight on the control effort and the miss distance
ξ	=	target-missile relative displacement normal to the initial LOS, m
$\gamma_{(\cdot)}$	=	flight-path angle, rad
Λ^j	=	jth regime conditioned likelihood function
μ^j	=	probability that the jth regime is correct
$\bar{\boldsymbol{\mu}}$	=	vector of posterior probabilities representing PN, APN, and OGL
$\boldsymbol{\nu}^j$	=	innovation sequence of the jth regime
$\sigma^2_{(\cdot)}$	=	measurement noise variance
θ	=	normalized time-to-go
λ	=	angle between the line of sight and the X_I axis, rad
$\varrho, \bar{\varrho}$	=	design parameters of the reduced-order approach
$\tau_{(\cdot)}$	=	first-order time constant, s
$\boldsymbol{\Phi}$	=	transition matrix
$\mathcal{N}$	=	Gaussian distribution
$\mathcal{U}$	=	set of possible missile guidance laws
$\tilde{(\cdot)}$	=	approximated value
$\hat{(\cdot)}$	=	estimated value
Subscripts		
0	=	initial values
k	=	step of the discrete time t_k
r, λ	=	along and normal to the line of sight
T, M, E	=	target, missile, and evasion, respectively
Superscripts		
j	=	jth regime/filter
$\perp$	=	normal to the initial line of sight
$*$	=	optimal solution

I. Introduction

Guidance laws for intercepting a moving target, such as aircraft in this study, have traditionally been developed for one-on-one engagements. Usually, optimal control theory is applied, and perfect information and linearized kinematics are assumed [1]. For example, proportional navigation (PN) is the optimal guidance law for a scenario between an attacking missile with ideal dynamics and a non-maneuvering target [2]. The same is true for augmented proportional navigation (APN), if the target performs a constant maneuver [3]. Taking into account first-order missile dynamics the well-known optimal guidance law (OGL) was obtained by Cottrell [4]. In [5], this work was extended to arbitrary known target maneuvers. All these guidance laws are linear and have the same general form of an effective navigation gain N' (constant or time-varying) multiplied by a zero-effort-miss term and divided by time-to-go squared.

In order to respond to the threat from homing missiles employing such guidance laws, a significant effort

was made to extend the protection capabilities of targeted aircrafts. Among the systems developed for this purpose are electronic countermeasures (e.g., jammers) and various kinds of decoys (chaff or flares). Besides these means of protection, an aircraft can perform an evasive maneuver, which can be either arbitrary or optimally adjusted against the incoming missile. In case of random maneuvers, two types are suggested: random telegraph [6, 7] and periodic sine or square wave maneuver with a random phase, in a frequency that is matched to the interceptor's navigation gain and time constant [8, 9].

It is also possible to develop an optimal evasion strategy using optimal control theory tools, however it requires information on the missile's future behavior, i.e., its guidance law and guidance parameters. Practically, it implies that the pilot is alerted that a missile of known type has been launched against his aircraft. A case study where such a problem was formulated as a one-sided optimal control problem against a PN-guided missile was presented in [10–12]. In these works some simplifying assumptions were applied, such as two dimensional analysis and constant pursuer and evader speeds with bounded maneuverabilities. Nonlinear engagement kinematics along with assumptions on first order missile dynamics were considered for the problem formulation in [11]. A numerical solution was presented over a set of various initial engagements conditions. In [12] a linearization around the collision course was made assuming ideal missile dynamics. This study was extended in [10] to a nonlinear model. The resulting optimal evasion strategies obtained in the above works were found to have a bang-bang structure, i.e. applying maximum available acceleration normal to the line of sight (LOS) for a given period of time.

Although there has been substantial work in the literature on target evasion, most of the research concentrated on PN guided interceptor missiles, which leaves the strategies against other missile guidance laws lacking. In a recent work of [13], optimal evasion strategies for a target aircraft from a homing missile employing a linear guidance law was derived. The problem was analyzed for arbitrary-order linear missile and target dynamics, bounded target controls, and assuming perfect information. The underlying assumption in this solution is that the missile's guidance strategy is exactly known to the target. Furthermore, the lack of appropriate guidance law and guidance parameter identification solutions greatly reduces the utility of the available target-evasion strategies.

Motivated to enhance aircraft survivability in situations where the relative state and the missile strategy are not exactly known, a multiple model adaptive evasion strategy is proposed which greatly relaxes the assumptions made in [13]. It is assumed that the missile is chasing the target using one of a finite set of linear guidance laws and guidance parameters, which is referred to as "regime" or "mode". Each such regime generates different missile acceleration commands and will therefore result in different missile trajectories. The active regime has to be identified first. In this paper, an extended Kalman filter (EKF) based multiple model adaptive estimator (MMAE) approach is used to identify the missile's active guidance strategy. Similar approach was used in [14] to design a cooperative multiple model guidance for an aircraft defending missile. In the MMAE approach, each model in this scheme represents a possible guidance law and corresponding guidance parameters of the attacking missile. The idea is to run a bank of filters in parallel, with each filter matching a different possible regime. The estimation is then a weighted sum of the state estimates from each individual filter in the bank, and the weights represent the probability of each regime being correct based on the measurement history. The regime probabilities at each time step are updated based on Bayesian inference, using the previous time step's regime probabilities and the regime-conditioned likelihood of the new measurement. For each considered regime, an optimal target evasion law is paired. Each optimal evasion law is derived based on a linearized model, but implemented in the nonlinear setting. The final optimal target maneuver is computed in a multiple model adaptive control (MMAC) framework using the posterior probabilities of each regime being correct. In the MMAC approach, the estimation of each elementary filter is fed into a "controller" (matched optimal evasion strategy in our case) matched to the filter's specific regime and the total scheme control command is then determined by the minimum mean square error (MMSE) criterion or maximum a posteriori probability (MAP) criterion. Additionally, a set of "classical" missile guidance laws such as PN, APN, and OGL, as well as the corresponding optimal evasion strategies from these laws are presented. For these classical guidance guidance laws, an alternative reduced-order approach is proposed to reduce the computational burden of the full-order MMAE. In this reduced-order approach, the number of MMAE regimes is reduced to maximum three. Each regime represents one of the classical guidance laws, i.e., PN, APN, or OGL. The corresponding guidance parameter is treated as an unknown parameter that has to be estimated.

From observability point of view, if only LOS angle measurements are available, the quality of the estimation of the relative state depends upon the intercept trajectory, which is reflected by the system

observability. For example, proportional navigation attempts to null the LOS rate and consequently range and range-rate are not observable [15]. So, in case of bearing-only measurements, the range can be hardly reconstructed from LOS measurements. This, in turn, might result in poor evasion performance. The bearing-only target tracking problem with application to missile guidance has been largely studied in the past [16–18]. Contrary, there exist only scarce open literature on guidance law and guidance parameter identification using bearing-only measurements. Nevertheless, identifying a highly maneuverable missile in the presence of missile maneuver uncertainty and noisy measurements is still a challenging problem and is limited by the estimation performance. A solution to improve range observability is to maneuver away from the collision triangle [19], this causes the LOS to rotate which then will give some insights on the relative range. These principles are also incorporated into the proposed evasion strategy.

The remainder of this paper is organized as follows. The next section presents the mathematical models of the missile-target engagement. The optimal target evasion strategy is presented in Sec. III, followed by the derivation of a multiple model adaptive control based evasion strategy in Sec. IV. A comprehensive performance analysis of the proposed approach is presented in Sec. VI, followed by concluding remarks.

II. Mathematical Models

This section presents the full nonlinear kinematics and dynamics equations of the missile-target evasion problem, which will serve for analysis. Then, linearized equations, used for the derivation of the optimal target evasion strategy, are presented. Measurement models and considered assumptions are also discussed.

A. Nonlinear Kinematics and Dynamics

The studied problem consists of two entities: an evading target aircraft and an attacking missile. Next, for brevity, the target aircraft is referred as target and the attacking missile as missile. The engagement will be analyzed in two-dimensions. In Figure 1 a schematic view of the planar point mass missile-target engagement geometry is shown, where X_I - O_I - Y_I represents a Cartesian inertial reference frame. The missile and target related variables are denoted by the subscripts M and T, respectively. The speed, acceleration, and flight-path angles are denoted by V, a, and γ, respectively; the range between the missile and target is r, and λ is the angle between the LOS and X_I axis.

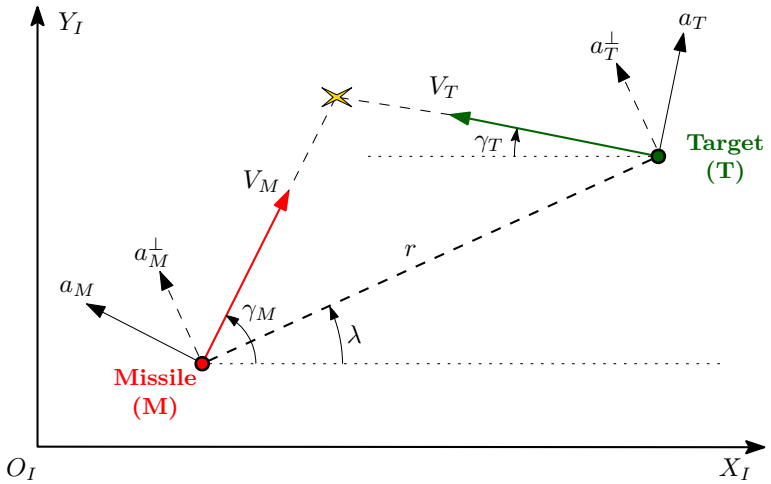

Figure 1: Planar missile-target engagement geometry

Neglecting the gravitational force, the engagement kinematics, expressed in a polar coordinate system (r, λ) attached to the missile, is:

$$\dot{r} = V_r, \tag{1}$$

$$\dot{\lambda} = V_\lambda / r, \tag{2}$$

where the relative velocities along and perpendicular to the LOS are

$$V_r = -V_M \cos(\gamma_M - \lambda) - V_T \cos(\gamma_T + \lambda), \tag{3}$$
$$V_\lambda = -V_M \sin(\gamma_M - \lambda) + V_T \sin(\gamma_T + \lambda). \tag{4}$$

The running time is denoted as t. The endgame initiates at $t = 0$ with $\dot{r}(t = 0) < 0$ and terminates at $t = t_f$, where

$$t_f = \underset{t}{\arg\inf}\{r(t)\dot{r}(t) = 0\}, \qquad t > 0, \tag{5}$$

allows to define the time-to-go by

$$t_{go} \triangleq t_f - t. \tag{6}$$

At $t = t_f$, the missile-target separation $r(t_f)$ is minimal and is often referred to as "miss distance".

During the endgame, the missile and the target are assumed to move at a constant speed and to perform lateral maneuvers only. Moreover, arbitrary-order linear missile and target dynamics are assumed, i.e.,

$$\begin{cases} \dot{\boldsymbol{y}}_i = \boldsymbol{A}_i \boldsymbol{y}_i + \boldsymbol{B}_i u_i \\ a_i = \boldsymbol{C}_i \boldsymbol{y}_i + d_i u_i \\ \dot{\gamma}_i = a_i / V_i \end{cases}, \qquad i = \{M, T\}, \tag{7}$$

where $\boldsymbol{y}_i \in \mathbb{R}^{n_i}$ is the internal state vector of the ith entity's dynamics, a_i and u_i are the ith entity's acceleration and acceleration command, respectively. It is also assumed that the target's maneuver capability is limited to $|u_T| \leq a_T^{max}$. In Eq. (7), the term $\boldsymbol{C}_i \boldsymbol{y}_i$ is denoted as a_{iS} and represents, if it exists, the part of the acceleration with dynamics (for example, an angle of attack generating lift). The second part of the acceleration, i.e. $d_i u_i$, represents the direct lift, which can be obtained immediately from deflection of the steering mechanism such as the canard or tail (neglecting servo dynamics).

The missile and target accelerations normal to the LOS, routinely used in guidance logic, are denoted by $a_M^\perp$ and $a_T^\perp$, respectively, satisfying

$$a_M^\perp = a_M \cos(\gamma_M - \lambda), \tag{8a}$$
$$a_T^\perp = a_T \cos(\gamma_T + \lambda). \tag{8b}$$

Note that in Eq. (7), and in the remainder of this paper, bold-italic is used to represent matrix or vector.

B. Linearized Equations of Motion

If during the endgame the missile and target deviations from the collision triangle are small, then the linearization around the initial LOS is justified [1]. In Fig. 2, the linearized planar geometry and the corresponding kinematics variables are depicted. The X-axis, aligned with the LOS used for linearization, is denoted as LOS_0. The relative displacement between the target and missile normal to this direction is ξ. Under linearization assumption, $a_M^\perp$ and $a_T^\perp$ are approximated by

$$a_M^\perp \approx k_M a_M, \qquad k_M = \cos(\gamma_{M0} - \lambda_0), \tag{9a}$$
$$a_T^\perp \approx k_T a_T, \qquad k_T = \cos(\gamma_{T0} + \lambda_0), \tag{9b}$$

where the subscript "0" denotes the initial value around which linearization has been performed. It is assumed that the missile is launched in a colison course, i.e., that $|\gamma_{M0} - \lambda_0| < \pi/2$ and $|\gamma_{T0} + \lambda_0| < \pi/2$.

During the endgame, the missile and target are assumed to move at a constant speed. Thus, once a collision triangle is reached and maintained, the speed V_r is constant and the interception time t_f can be assumed fixed and approximated by

$$\tilde{t}_f \approx -r_0 / V_r \tag{10}$$

Let us define the state vector $\boldsymbol{y}$ of the linearized missile-target evasion problem as

$$\boldsymbol{y} = \begin{bmatrix} y_1 & y_2 & \boldsymbol{y}_M^T & \boldsymbol{y}_T^T \end{bmatrix}^T \triangleq \begin{bmatrix} \xi & \dot{\xi} & \boldsymbol{y}_M^T & \boldsymbol{y}_T^T \end{bmatrix}^T.$$

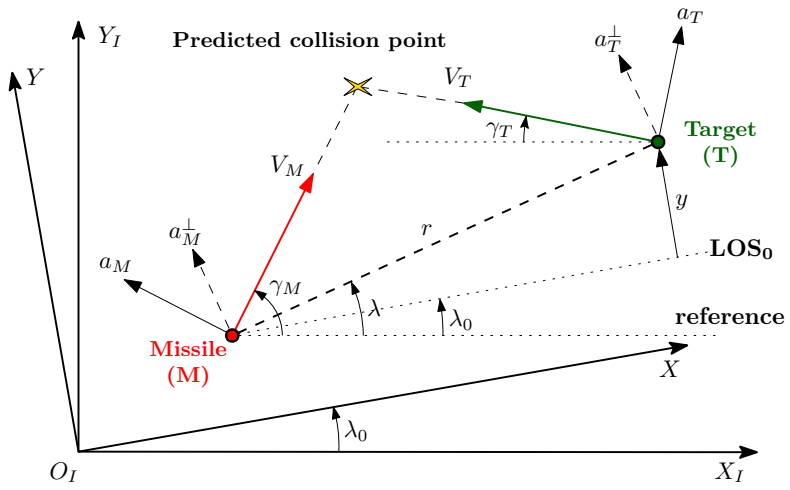

Figure 2: Linearized planar missile-target engagement geometry

Then, the missile-target equations of relative motion normal to LOS$_0$ can be expressed as

$$\begin{cases} \dot{y}_1 = y_2 \\ \dot{y}_2 = k_T a_T - k_M a_M \\ \dot{\boldsymbol{y}}_M = \boldsymbol{A}_M \boldsymbol{y}_M + \boldsymbol{B}_M u_M \\ \dot{\boldsymbol{y}}_T = \boldsymbol{A}_T \boldsymbol{y}_T + \boldsymbol{B}_T u_T \end{cases} \tag{11}$$

Using Eqs. (7) and (9), the above equations can be rewritten into a matrix form as

$$\dot{\boldsymbol{y}} = \boldsymbol{A}\boldsymbol{y} + \boldsymbol{B}u_T^\perp + \boldsymbol{C}u_M^\perp, \tag{12}$$

$$\boldsymbol{A} = \begin{bmatrix} 0 & 1 & [0]_{1\times n_M} & [0]_{1\times n_T} \\ 0 & 0 & -k_M \boldsymbol{C}_M & k_T \boldsymbol{C}_T \\ [0]_{n_M\times 1} & [0]_{n_M\times 1} & \boldsymbol{A}_M & [0]_{n_M\times n_T} \\ [0]_{n_T\times 1} & [0]_{n_T\times 1} & [0]_{n_T\times n_M} & \boldsymbol{A}_T \end{bmatrix}, \quad \boldsymbol{B} = \begin{bmatrix} 0 \\ d_T \\ [0]_{n_M\times 1} \\ k_T^{-1}\boldsymbol{B}_T \end{bmatrix}, \quad \boldsymbol{C} = \begin{bmatrix} 0 \\ -d_M \\ k_M^{-1}\boldsymbol{B}_M \\ [0]_{n_T\times 1} \end{bmatrix},$$

where $[0]$ denotes a matrix of zeros with a given dimension, $u_M^\perp$ and $u_T^\perp$ being, respectively, the missile and target acceleration commands normal to LOS$_0$. Note that the command $u_i^\perp, i \in \{M, T\}$ is related to u_i analogously as $a_i^\perp$ is related to a_i, see Eqs. (8) and (9).

C. Measurement Model

The target is assumed to be equipped with an electro-optic seeker and/or a radar. Thus, one may measure: *a*) both r and λ, or *b*) only λ, i.e., bearing-only measurement. The discrete-time measurement vector $\boldsymbol{z}_k \in \mathbb{R}^{n_z}$ is assumed to be acquired at a given sampling time T_s^m and being corrupted by a zero-mean mutually independent white Gaussian noise sequence $\boldsymbol{v}_k \in \mathbb{R}^{n_z}$. The measurement model, when all possible measurements are available, is

$$\boldsymbol{z}_k = \boldsymbol{H}\boldsymbol{x}_k + \boldsymbol{v}_k = \begin{bmatrix} r_k \\ \lambda_k \end{bmatrix} + \boldsymbol{v}_k, \tag{13}$$

where

$$\boldsymbol{v}_k \sim \mathcal{N}([0]_{n_z\times 1}, \boldsymbol{R}), \qquad \boldsymbol{R} = \mathrm{diag}(\sigma_r^2, \sigma_\lambda^2),$$

$\boldsymbol{x}_k$ is the relevant state vector (being defined later) at discrete time t_k, and $\boldsymbol{H}$ is the appropriate measurement matrix. If r_k is not available, the appropriate row is eliminated from $\boldsymbol{H}$ and the appropriate row and column are eliminated from $\boldsymbol{R}$, respectively.

III. Optimal Target Evasion

In this section, the nonlinear implementation of the optimal target evasion strategy from a missile employing a linear guidance law is presented.

A. Missile Guidance Law

In this paper, a family of linear guidance laws, commonly derived under the assumption of linear kinematics, perfect information, and unbounded controls, is considered [1]. This common practice resulted in a class of guidance laws, which all have the same linear form as a function of the missile-target linear state $\boldsymbol{y}$ and eventually the target's control $u_T^{\perp}$, i.e.,

$$u_M^{\perp} = \boldsymbol{K}(t_{go})\boldsymbol{y} + K_{u_T}(t_{go})u_T^{\perp}, \tag{14}$$

where

$$\boldsymbol{K}(t_{go}) = \begin{bmatrix} K_1 & K_2 & \boldsymbol{K}_M & \boldsymbol{K}_T \end{bmatrix}.$$

Note that Eq. (14) represents a wide variety of linear guidance laws. In the next two sections, a set of "classical" missile guidance laws such as PN, APN, and OGL as well as the corresponding optimal evasion strategies from these laws will be presented.

Remark 1. *In Eq.* (14)*, it is assumed that the missile's current controller may be dependent on the target's current controller. Actually, if the missile uses an optimal-control based guidance law, then the underlying assumption in its derivation was that the target's controller is known not just at the current time but also from the current time until the end of the scenario [13].*

B. Optimal Evasion Problem - Linear Setting

Using the equations of motion (EOM) of the linearized missile-target engagement, see Eq. (12), together with the general form of the linear missile guidance law, see Eq. (14), the EOM of the one-sided evasion problem are obtained

$$\dot{\boldsymbol{y}} = \boldsymbol{A}_E(t_{go})\boldsymbol{y} + \boldsymbol{B}_E(t_{go})u_T^{\perp}, \tag{15}$$

where

$$\boldsymbol{A}_E(t_{go}) = \begin{bmatrix} 0 & 1 & [0]_{1\times n_M} & [0]_{1\times n_T} \\ -d_M K_1 & -d_M K_2 & -k_M \boldsymbol{C}_M - d_M \boldsymbol{K}_M & k_T \boldsymbol{C}_T - d_M \boldsymbol{K}_T \\ k_M^{-1}\boldsymbol{B}_M K_1 & k_M^{-1}\boldsymbol{B}_M K_2 & \boldsymbol{A}_M + k_M^{-1}\boldsymbol{B}_M \boldsymbol{K}_M & k_M^{-1}\boldsymbol{B}_M \boldsymbol{K}_T \\ [0]_{n_T\times 1} & [0]_{n_T\times 1} & [0]_{n_T\times n_M} & \boldsymbol{A}_T \end{bmatrix},$$

$$\boldsymbol{B}_E(t_{go}) = \begin{bmatrix} 0 & d_T - d_M K_{u_T} & k_M^{-1}\boldsymbol{B}_M^T K_{u_T} & k_T^{-1}\boldsymbol{B}_T^T \end{bmatrix}^T.$$

Based on Eq. (15), the optimal target evasion strategy from Eq. (14) has been derived in [13] and is briefly recalled in the following theorem.

Theorem 1. The optimal target evasion strategy from a homing missile employing a linear guidance law of the form of Eq. (14), maximizing the following cost function

$$J_E = y_1^2(t_f)/2 \tag{16}$$

subject to the EOM of of Eq. (15) and under the constraint that the target's control $|u_T| \leq a_T^{max}$ is bounded, is given by

$$u_T^{\perp *} = a_T^{\perp max}\text{sign}(s_{MT})\text{sign}(Z_{MT}), \qquad Z_{MT}(0) \neq 0, \tag{17}$$

where s_{MT} is the switching function and Z_{MT} is the well-known zero-effort-miss (ZEM) distance given by, respectively,

$$s_{MT} = \boldsymbol{D}_E \boldsymbol{\Phi}_E(t_f, t)\boldsymbol{B}_E(t_{go}), \tag{18}$$

$$Z_{MT} = \boldsymbol{D}_E \boldsymbol{\Phi}_E(t_f, t)\boldsymbol{y}, \tag{19}$$

and $\boldsymbol{D}_E$ being a constant vector

$$\boldsymbol{D}_E = \begin{bmatrix} 1 & 0 & [0]_{1\times n_M} & [0]_{1\times n_T} \end{bmatrix}. \tag{20}$$

The transition matrix $\boldsymbol{\Phi}_E(t_f, t)$, associated with the homogenous solution of Eq. (15), having the structure

$$\boldsymbol{\Phi}_E(t_f, t) = \boldsymbol{\Phi}_E(t_{go}) = \begin{bmatrix} \Phi_{11} & \Phi_{12} & \boldsymbol{\Phi}_{1M} & \boldsymbol{\Phi}_{1T} \\ \Phi_{21} & \Phi_{22} & \boldsymbol{\Phi}_{2M} & \boldsymbol{\Phi}_{2T} \\ \boldsymbol{\Phi}_{31} & \boldsymbol{\Phi}_{32} & \boldsymbol{\Phi}_{3M} & \boldsymbol{\Phi}_{3T} \\ \boldsymbol{\Phi}_{41} & \boldsymbol{\Phi}_{42} & \boldsymbol{\Phi}_{4M} & \boldsymbol{\Phi}_{4T} \end{bmatrix}, \tag{21}$$

satisfies

$$\dot{\boldsymbol{\Phi}}_E(t_f, t) = -\boldsymbol{\Phi}_E(t_f, t)\boldsymbol{A}_E(t_{go}), \qquad \boldsymbol{\Phi}_E(t_f, t_f) = \boldsymbol{I}. \tag{22}$$

In Eq. (17), $a_T^{\perp max}$ is a projection of the target's maximum lateral acceleration a_T^{max} in the direction perpendicular to LOS_0, and is given by: $a_T^{\perp max} = k_T a_T^{max}$.

Proof. The proof of Theorem 1 can be found in [13]. □

Remark 2. *If the engagement is initialized in the singular region, i.e., $Z_{MT}(0) = 0$, or if $Z_{MT}(t) = 0$, $t > 0$, then it was suggested in [13] that the optimal evasion strategy $u_T^{\perp *}$ should be chosen as either $a_T^{\perp max}$ or $-a_T^{\perp max}$. In fact, if the missile employs OGL homing strategy with $\alpha = 0$ (for more details about α, see the discussion in Sec. IVB), then the target has no chance to escape and thus $Z_{MT}(t) = 0$ for any t.*

It was also shown in [13] that if the optimal evasion strategy $u_T^{\perp *}$ is used within the linear setting, the optimal ZEM dynamics, i.e., $\dot{Z}_{MT}^*$, is governed by

$$\dot{Z}_{MT}^* = \mathrm{sign}(Z_{MT})\,|s_{MT}|\,a_T^{\perp max}. \tag{23}$$

Consequently, $|Z_{MT}|$ is a monotonically increasing function of time, satisfying $\forall t \in [0, t_f]$

$$\mathrm{sign}(Z_{MT}(t)) = \mathrm{sign}(Z_{MT}(t_f)), \qquad Z_{MT}(0) \neq 0. \tag{24}$$

Defining $m = \int_0^{t_f} |s_{MT}| a_T^{\perp max} dt$, the expected (under the assumption of linearity) miss distance is obtained as follows

$$\mathrm{Miss}_{(\mathrm{exp})} = |y_1(t_f)| = |Z_{MT}(t_f)| = |Z_{MT}(0)| + m. \tag{25}$$

The consequence of Eq. (24) is that Z_{MT} does not change its sign during the engagement. Therefore, if $Z_{MT}(0) \neq 0$ is known, the only parameter needed for the computation of the optimal target control $u_T^{\perp *}$ is the time-to-go t_{go} that is used to evaluate the sign of switch function $s_{MT}(t_{go})$. However, this is only valid if the linearization assumptions hold.

Remark 3. *The optimal target evasion strategy of Eq. (17) was derived under the assumption of unbounded missile control command $u_M^{\perp}$. It was shown in [12] that if the missile acceleration $a_M^{\perp}$ or $u_M^{\perp}$ are bounded, then in order to exploit the missile's saturation the target maneuver switches should occur earlier in the engagement.*

C. Nonlinear Implementation

Based on Theorem 1, the target's optimal evasion strategy is a closed-loop guidance law in which the target needs to compute $s_{MT}(t_{go})$ and $Z_{MT}(t)$. These variables are in general functions of the time-to-go t_{go} and the linear state $\boldsymbol{y}$. To implement such evasion strategy within the nonlinear setting, $u_T^{\perp *}$ must be projected in the direction normal to the target's velocity vector, denoted as u_T^*. Assuming small deviations from the collision triangle leads to $k_T/\cos(\gamma_T + \lambda) \approx 1$, hence u_T^* can be approximated as

$$u_T^* = \frac{u_T^{\perp *}}{\cos(\gamma_T + \lambda)} \approx a_T^{max}\mathrm{sign}(s_{MT})\mathrm{sign}(Z_{MT}), \qquad Z_{MT}(0) \neq 0. \tag{26}$$

Once a collision triangle is reached and maintained, the speed V_r is constant and the approximation of the interception time $\tilde{t}_f$, given by Eq. (10), can be assumed fixed throughout the engagement. Therefore, the relevant components of $\boldsymbol{\Phi}_E(\tilde{t}_f, t)$, needed to determine $s_{MT}(t_{go})$, can be precomputed off-line.

Note that Z_{MT}, given by Eq. (19), is a function of the linear state $\boldsymbol{y}$. The displacement ξ normal to LOS_0 can be expressed at any time by

$$\xi = r\sin(\tilde{\lambda}), \tag{27}$$

where $\tilde{\lambda} = \lambda - \lambda_0$. Differentiating Eq. (27) with respect to time, yields

$$\dot{\xi} = V_r \sin(\tilde{\lambda}) + V_\lambda \cos(\tilde{\lambda}). \tag{28}$$

Using the above expressions, Eqs. (27) and (28), for the computation of Z_{MT} replaces the dependency on ξ and $\dot{\xi}$ by the kinematics variables V_r, V_λ, r, and λ. Moreover, assuming small deviations from the collision triangle, thus $\lambda - \lambda_0 \approx 0$, the relative displacement ξ can be assumed zero and the time derivative $\dot{\xi}$ can be approximated as $\dot{\xi} = V_\lambda$.

Remark 4. *As outlined previously, $|Z_{MT}|$ is monotonically increasing in time only if the linearity assumptions hold. If these assumptions are violated or if uncertain states are used to compute Z_{MT}, then Z_{MT} might change its sign during the evasion. Such phenomena might result in unnecessary switches of u_T^*, which consequently might lead to undesired reduction in the resulting miss distance. This phenomena is obviously not appreciated and a workaround will be discussed in Sec. VD.*

Remark 5. *It is obvious that if the collision triangle changes its geometry throughout the engagement (requiring relinearization), the transition matrix $\boldsymbol{\Phi}_E(t_{go})$, used to determine the optimal switches $s_{MT}(t_{go})$ and the ZEM distance $Z_{MT}(t)$, is not necessary the optimal transition matrix. Thus, one may consider to recompute $\boldsymbol{\Phi}_E(t_{go})$ every time when a significant change in the linearized collision geometry is observed.*

IV. MMAE for Missile Identification

The underlying assumption of Theorem 1 is that the missile's guidance strategy is exactly known to the target. In this section, based on Magill's pioneering work [20], a multiple model online identification scheme is proposed to identify the employed missile guidance law and all the parameters (relative state and time-to-go) required for the proper implementation of the evasion strategy given in Sec. V. The set of "classical" missile guidance laws, used to validate the proposed evasion strategy in Sec. VI, is also presented. Finally, an alternative reduced-order approach is proposed to save computational resources.

A. Multiple Model Adaptive Estimation

In the multiple model estimation approach, it is assumed that the system operates in one of a finite number of models. The operating model is often called as *mode* or *regime* of the system. If the regime that the system obeys is fixed, that is, no switching from one mode to another occurs during the estimation process, then the static multiple model estimator, also known as the MMAE approach, is considered [20, 21]. While the model that is in effect stays fixed, each model has its own dynamics, so the overall estimator is dynamic.

Let's assume that the guidance strategy u_M of the missile, being fixed throughout the engagement, is one of p possible ones (the system operates in one of p regimes)

$$u_M \in \mathcal{U} = \{u_M^1, \ldots, u_M^p\}. \tag{29}$$

Each guidance strategy u_M^j is characterized by a set of five parameters $\{K_1^j, K_2^j, \boldsymbol{K}_M^j, \boldsymbol{K}_T^j, K_{u_T}^j\}$. These parameters exclusively define the jth regime and can be functions of t_{go}. Each such regime will generate different missile acceleration commands u_M, defined by the linear guidance law of Eq. (14), and therefore will result in different missile trajectories. If the target-related parameters such as $\boldsymbol{y}_T$, γ_T, and V_T are assumed to be known to a very high accuracy (via some navigation system), then, based on the constant missile speed assumption, the jth regime dynamics is governed by the following set of nonlinear equations

$$\begin{cases} \dot{r} &= V_r \\ \dot{\lambda} &= V_\lambda / r \\ \dot{\boldsymbol{y}}_M &= \boldsymbol{A}_M \boldsymbol{y}_M + \boldsymbol{B}_M u_M^j \\ \dot{\gamma}_M &= (\boldsymbol{C}_M \boldsymbol{y}_M + d_M u_M^j)/V_M \\ \dot{V}_M &= 0 \end{cases}, \tag{30}$$

where V_r and V_λ are given by Eqs. (3) and (4), respectively, and u_M^j is the missile's acceleration command obeying the jth regime defined using Eqs. (14),(27),(28) and (8a) as

$$u_M^j = \frac{K_1^j r \sin(\tilde{\lambda}) + K_2^j \left(V_r \sin(\tilde{\lambda}) + V_\lambda \cos(\tilde{\lambda})\right) + \boldsymbol{K}_M^j \boldsymbol{y}_M + \boldsymbol{K}_T^j \boldsymbol{y}_T + K_{u_T}^j u_T^\perp}{\cos(\gamma_M - \lambda)}. \tag{31}$$

The discrete-time version of Eq. (30), used for MMAE design, can be compactly rewritten as

$$\boldsymbol{x}_k = \boldsymbol{f}_{k-1}^j(\boldsymbol{x}_{k-1}, u_T^\perp), \tag{32}$$

where $\boldsymbol{x}_k \triangleq [r, \lambda, \boldsymbol{y}_M^T, \gamma_M, V_M]^T$ is the state vector at time $t_k = kT_s$, $T_s > 0$ used for estimation, $\boldsymbol{f}_{k-1}^j$ is a vector function derived by integrating of Eq. (30) from t_{k-1} to t_k, and j is the particular regime.

Remark 6. *In the above model, an assumption has been made that the parameters of the missile dynamics, i.e., $\boldsymbol{A}_M$, $\boldsymbol{B}_M$, $\boldsymbol{C}_M$, and d_M, are known exactly. If this is not the case, the missile dynamics can be approximated by e.g., a first-order strictly proper dynamics, i.e., $\boldsymbol{A}_M = -1/\tau_M$, $\boldsymbol{B}_M = 1/\tau_M$, $\boldsymbol{C}_M = 1$, $d_M = 0$, and the uncertainty on τ_M can be treated in two different ways: a) several values of τ_M can be represented as different regimes and the problem can be addressed in the same way as the guidance law uncertainty is addressed, or b) τ_M can be added as a constant state in Eq.* (30) *similarly as V_M.*

As the engagement model in Eq. (30) is nonlinear, a mode-matched EKF is used to calculate the state estimate, $\hat{\mathbf{x}}^j$, and the associated regime probability, μ^j, assuming the jth regime being correct, see [14] for more details. Note that other nonlinear filtering techniques, such as particle filter [22] or unscented Kalman filter [23], can be utilized for this purpose as well. The main idea is to design and run in parallel a bank of p filters, each matching a different regime j. Then, the regime probabilities at each time step are calculated based on Bayesian inference, using the previous time step's regime probabilities (weights) and the mode-conditioned likelihood of the new measurement. Starting with the initial probability μ_0^j that u_M^j is correct (missile employs u_M^j), i.e.,

$$\text{Prob}\{u_M^j | \mathcal{Z}_0\} = \mu_0^j, \qquad \forall j \in \{1, \ldots, p\}, \tag{33}$$

where $\mathcal{Z}_0$ is some information known a priori, $\sum_{j=1}^p \mu_0^j = 1$ since the correct law is among the assumed p possible ones, then using Bayes' rule, the posterior probability, given the measurement data $\mathbf{z}_{1:k} \triangleq \{\mathbf{z}_i; i = 1, \ldots, k\}$ up to time k μ_k^j, is given by the recursion [21]

$$\mu_k^j \triangleq \text{Prob}\{u_M^j | \boldsymbol{z}_{1:k}\} = \frac{p(\boldsymbol{z}_k | \boldsymbol{z}_{1:k-1}, u_M^j) \text{Prob}\{u_M^j | \boldsymbol{z}_{1:k-1}\}}{p(\boldsymbol{z}_k | \boldsymbol{z}_{1:k-1})}. \tag{34}$$

Using the initial probabilities of Eq. (33) and applying the total probability of Eq. (34) results in the following weight update formula for time k

$$\mu_k^j = \frac{\Lambda_k^j \mu_{k-1}^j}{\sum_{i=1}^{n_r} \Lambda_k^i \mu_{k-1}^i}, \qquad \forall j \in \{1, \ldots, p\}, \tag{35}$$

where $\Lambda_k^j \triangleq p(\boldsymbol{z}_k | \boldsymbol{z}_{1:k-1}, u_M^j)$ is the jth regime-conditioned likelihood function calculated using the jth filter innovations process statistics. Under the linear-Gaussian assumptions, Λ_k^j is Gaussian and given by

$$\Lambda_k^j = p(\boldsymbol{\nu}_k^j) = \mathcal{N}(\boldsymbol{\nu}_k^j; [0]_{n_z \times 1}, \boldsymbol{S}_k^j), \tag{36}$$

where $\boldsymbol{\nu}_k^j$ and $\boldsymbol{S}_k^k$ are the innovation and its covariance from the jth mode-matched filter. It is obvious that $\mu_k^j \geq 0$ and that $\sum_{i=1}^p \mu_k^i = 1$. In a nonlinear and/or non-Gaussian setting, Gaussian likelihood functions are used, although they are clearly approximations [21].

Remark 7. *The fixed missile guidance law assumption, i.e., that the missile does not switch between guidance laws throughout the engagement, is a very realistic assumption for the endgame. If this assumption does not hold, a dynamic multiple model estimator can be derived based on the interacting multiple model (IMM) approach [18, 21]. The IMM allows transitions between regimes, but the probabilities of these transitions are needed to be known.*

B. MMAE for Classical Missile Guidance Laws

Among the large family of linear guidance laws, special attention is given here to the most well-known guidance laws of PN [2], APN [3], and OGL [4]. These guidance laws are more widely known in the following nonlinear form: (rather than in the form of Eq. (31))

$$u_M^i = N_i' \frac{Z_i}{t_{go}^2 \cos(\gamma_M - \lambda)}, \qquad i \in \{\text{PN}, \text{APN}, \text{OGL}\}, \tag{37}$$

where N' is the effective navigation gain and Z is the missile's ZEM distance. The expression for the ZEM distance is different for each guidance law, as it is dependent on the model used and assumptions made regarding the future target maneuvers.

Remark 8. *In the above context, the ZEM represents the missile-target separation normal to LOS_0 at the final time t_f, i.e., $y_1(t_f) = \xi(t_f)$, which will be obtained if the attacking missile does not apply any control from the current time onward and the target aircraft continues employing the expected maneuver strategy that is known to the missile.*

• *PN-Guided Missile*

Under the assumptions of ideal missile dynamics and no target maneuver (i.e., $u_T^{\perp}(t) = 0, \forall t \geq 0$), the obtained missile guidance law guaranteeing zero miss distance is PN with

$$Z_{PN} = -V_r t_{go}^2 \dot{\lambda}, \tag{38}$$

where $\dot{\lambda}$ is given by Eq. (2). If $N'_{PN} = 3$, this guidance law minimizes the control effort.

• *APN-Guided Missile*

Extending the results to the case in which the target is assumed to perform a constant maneuver (i.e., $u_T^{\perp}(t) = \text{const.}, \forall t \geq 0$), APN was obtained with

$$Z_{APN} = Z_{PN} + a_T \cos(\gamma_T + \lambda) t_{go}^2/2. \tag{39}$$

• *OGL-Guided Missile*

Additionally assuming that the missile's closed-loop acceleration dynamics can be approximated by a first-order strictly proper transfer with a time constant τ_M, OGL was obtained with

$$Z_{OGL} = Z_{APN} - \tau_M^2 \delta(\theta) a_{MS} \cos(\gamma_M - \lambda), \tag{40}$$

where the normalized time-to-go θ and the function $\delta(\theta)$ being

$$\theta = t_{go}/\tau_M, \tag{41}$$

$$\delta(\theta) = e^{-\theta} + \theta - 1. \tag{42}$$

The navigation gains of PN and APN are constant, whereas that of OGL is time-varying, i.e.,

$$N'_{OGL}(\theta) = \frac{6\theta^2 \delta(\theta)}{3 + 6\theta - 6\theta^2 + 2\theta^3 - 3e^{-2\theta} - 12\theta e^{-\theta} + 6\alpha/\tau_M^3}, \tag{43}$$

where α represents the ratio between the weights on the control effort (integral of the acceleration command squared) and the miss distance in the quadratic cost function J_{OGL} used in the OGL formulation:

$$J_{OGL} = \frac{b}{2} y_1^2(t_f) + \frac{1}{2} \int_0^{t_f} \left(u_M \cos(\gamma_{M0} - \lambda_0)\right)^2 dt, \qquad b \triangleq 1/\alpha. \tag{44}$$

Note, letting $\alpha \to 0$ yields to a perfect intercept requirement. If the missile has a first-order strictly proper dynamics and if the missile will be provided perfect (or even relatively precise) measurements on

the relative state, then the target has no chance to escape, no matter what maneuver it applies or what the initial conditions are. This is because OGL was designed taking into account such missile dynamics and assuming unbounded control [13]. In such a case, the aircraft survivability can be enhanced only by denying the missile such "perfect" information or by using a defender missile to intercept the incoming thread [13, 14, 24]. Therefore, the case when $\alpha = 0$ is out of scope of this paper.

In order to fit the classical guidance laws, introduced earlier, into the MMAE scheme of Sec. IVA, it is required to define a set $\mathcal{U}_c$ of possible regimes, as in Eq. (29), as follows

$$\mathcal{U}_c = \left\{ u_M^{PN}\left(N'_{PN} \in \bar{\boldsymbol{N}}'_{PN}\right),\ u_M^{APN}\left(N'_{APN} \in \bar{\boldsymbol{N}}'_{APN}\right),\ u_M^{OGL}\left(\alpha \in \bar{\boldsymbol{\alpha}}\right) \right\}, \tag{45}$$

where

$$\bar{\boldsymbol{N}}'_{PN} = \{N'^{(1)}_{PN}, \ldots, N'^{(p_1)}_{PN}\}, \quad \bar{\boldsymbol{N}}'_{APN} = \{N'^{(1)}_{APN}, \ldots, N'^{(p_2)}_{APN}\}, \quad \bar{\boldsymbol{\alpha}} = \{\alpha^{(1)}, \ldots, \alpha^{(p_3)}\}$$

represent the sets of considered navigation gains for PN and APN and the set of α parameters for OGL. Overall there are $p = \sum_{i=1}^{3} p_i$ regimes. For each regime it is necessary to construct the mode-matched EKF and run all the p filters in parallel.

C. Reduced Order MMAE for Classical Missile Guidance Laws

It is obvious that if the total number of considered regimes p is too large, it might pose some severe computational challenges. Identification of the above presented classical missile guidance laws requires the identification of the ZEM (either Z_{PN}, Z_{APN}, or Z_{OGL}) and the navigation gain (either N'_{PN}, N'_{APN}, or N'_{OGL}). With regards to the navigation gain, in the case of PN and APN the requirement is to identify its constant value, whereas for OGL the requirement is to identify α. This special structure of the classical guidance laws, see Eq. (37), allows to reduce the computational burden of the MMAE algorithm by reducing the total number of regimes to $p = 3$. Thus, a reduced set $\mathcal{U}_c^r$ of possible regimes is defined as follows

$$\mathcal{U}_c^r = \left\{ u_M^{PN}\left(N'_{PN}\right),\ u_M^{APN}\left(N'_{APN}\right),\ u_M^{OGL}\left(\alpha\right) \right\}, \tag{46}$$

where the guidance parameters N'_{PN}, N'_{APN}, and α are treated as unknown system parameters that need to be estimated. This can be easily incorporated into the existing MMAE scheme of Sec. IVA by adding, respectively, N'_{PN}, N'_{APN}, and α as a constant state (similarly as the constant missile speed V_M, i.e., $\dot{V}_M = 0$) into the EOM given by Eq. (30) for each regime. For more details on parameter estimation see e.g., [21].

V. Multiple Model Adaptive Evasion

In this section, the proposed MMAE scheme of Sec. IV and the optimal target evasion strategy of Sec. III are combined in a MMAC (multiple model adaptive control) configuration, followed by the derivation of specific optimal target evasions from the classical missile guidance laws. Finally, the MMAC adaptation to the reduced-order problem of Sec. IVC is given and some implementation issues are discussed.

A. MMAC-based Target Evasion

In the MMAC approach [25], the state estimate of each elementary filter is fed into the "controller" which is paired with the filter's specific regime. In our case, the paired "controller" corresponds to the optimal evasion strategy matched to the filter's particular regime. This framework fits our missile-target evasion problem as each regime j in the MMAE approach of Sec. IVA corresponds to a known missile strategy u_M^j, thus an optimal evasion strategy u_T^{*j}, matching u_M^j, can be easily derived based on developments presented in Sec. III. Finally, the total target control command u_T is determined in the MMAC sense by one of the following approaches: *a*) MMSE - minimum mean square error, or *b*) MAP - maximum a posteriori probability.

In the MMSE approach, u_T is a weighted average of controls from each filter-matched controller in the bank. The weighting is based on filter-matched controller's posterior probabilities μ_k^j, $j = 1, \ldots, p$. The target acceleration command at time step k can therefore be calculated as

$$u_T^{(mmse)} = \sum_{j=1}^{p} \mu_k^j u_T^{*j}, \tag{47}$$

where

$$u_T^{*j} = a_T^{max}\text{sign}(s_{MT}^j)\text{sign}(Z_{MT}^j), \tag{48}$$

s_{MT}^j and Z_{MT}^j represent, respectively, the switching function of Eq. (18) and the ZEM distance of Eq. (19) of the jth regime, both evaluated using the jth regime-conditioned state estimate $\hat{\boldsymbol{x}}_{k|k}^j$ at time step k.

In the MAP criterion sense, u_T is determined as the control associated with the maximum a posteriori probability, i.e.,

$$u_T^{(map)} = u_T^{*j}, \qquad j = \underset{i\in\{1,\ldots,p\}}{\text{argmax}}\,(\mu_k^i). \tag{49}$$

Note that unlike the MMAE approach, the MMAC approach is heuristic (an approximation), but seems to yield good performance when a controller can be matched to each possible regime [14, 26].

B. Optimal Evasion from Classical Missile Guidance Laws

Here, specific optimal target evasion strategies, matched against the classical missile guidance laws of PN, APN and OGL, are derived. The derivation can be extended to other missile guidance laws using the same formulation and similar derivation steps, unless they comply with the linear form of Eq. (14).

First, u_M of Eq. (37) need to be expressed in the general linear form $u_M^{\perp}$ of Eq. (14) which was used in the derivation of the optimal evasion strategy in Theorem 1. Assuming small deviations from the collision triangle, the displacement ξ normal to LOS_0 can be approximated by

$$\xi \approx r(\lambda - \lambda_0) \tag{50}$$

Differentiating Eq. (50) with respect to time yields

$$\xi + \dot{\xi}t_{go} = -V_r t_{go}^2 \dot{\lambda}. \tag{51}$$

It can be seen that the right hand side of Eq. (51) is actually identical with the expression for Z_{PN} in Eq. (38). Armed with the above expression, $\boldsymbol{K}(t_{go}) = [K_1 \quad K_2 \quad \boldsymbol{K}_M \quad \boldsymbol{K}_T]$ and K_{u_T} can be easily defined for PN, APN, and OGL-guided missiles as follows:

- *Evasion from PN-Guided Missile*

$$K_1 = \tfrac{N'_{PN}}{t_{go}^2}, \quad K_2 = \tfrac{N'_{PN}}{t_{go}}, \quad \boldsymbol{K}_M = [0]_{1\times n_M}, \quad \boldsymbol{K}_T = [0]_{1\times n_T}, \quad K_{u_T} = 0.$$

- *Evasion from APN-Guided Missile*

$$K_1 = \tfrac{N'_{APN}}{t_{go}^2}, \quad K_2 = \tfrac{N'_{APN}}{t_{go}}, \quad \boldsymbol{K}_M = [0]_{1\times n_M}, \quad \boldsymbol{K}_T = k_T\tfrac{N'_{APN}\mathbf{C}_T}{2}, \quad K_{u_T} = \tfrac{N'_{APN}d_T}{2}.$$

- *Evasion from OGL-Guided Missile*

$$K_1 = \tfrac{N'_{OGL}(\theta)}{t_{go}^2}, \quad K_2 = \tfrac{N'_{OGL}(\theta)}{t_{go}}, \quad K_{u_T} = \tfrac{N'_{OGL}(\theta)d_T}{2},$$
$$\boldsymbol{K}_M = -k_M\tfrac{N'_{OGL}(\theta)\delta(\theta)\mathbf{C}_M}{\theta^2}, \quad \boldsymbol{K}_T = k_T\tfrac{N'_{OGL}(\theta)\mathbf{C}_T}{2}.$$

Now, for all $u_M^j \in \mathcal{U}_c$ (or $u_M^j \in \mathcal{U}_c^r$, if the guidance parameter N' or α is known/identified), the optimal switching function s_{MT}^j and the ZEM distance function Z_{MT}^j can be determined by solving the following set of differential equations in reverse time:

$$\begin{cases} \dfrac{d\Phi_{11}}{dt_{go}} = \boldsymbol{\Phi}_{1M}k_M^{-1}\boldsymbol{B}_M K_1 - \Phi_{12}d_M K_1, & \Phi_{11}(0) = 1 \\ \dfrac{d\Phi_{12}}{dt_{go}} = \boldsymbol{\Phi}_{1M}k_M^{-1}\boldsymbol{B}_M K_2 + \Phi_{11} - \Phi_{12}d_M K_2, & \Phi_{12}(0) = 0 \\ \dfrac{d\boldsymbol{\Phi}_{1M}}{dt_{go}} = \boldsymbol{\Phi}_{1M}(\boldsymbol{A}_M + k_M^{-1}\boldsymbol{B}_M\boldsymbol{K}_M) - \Phi_{12}(k_M\boldsymbol{C}_M + d_M\boldsymbol{K}_M), & \Phi_{1M}(0) = [0]_{1\times n_M} \\ \dfrac{d\boldsymbol{\Phi}_{1T}}{dt_{go}} = \boldsymbol{\Phi}_{1M}k_M^{-1}\boldsymbol{B}_M\boldsymbol{K}_T + \boldsymbol{\Phi}_{1T}\boldsymbol{A}_T + \Phi_{12}(k_T\boldsymbol{C}_T - d_M\boldsymbol{K}_T), & \Phi_{1T}(0) = [0]_{1\times n_T}. \end{cases} \tag{52}$$

It can be noticed that in the above cases $K_2 = K_1 t_{go}$ and that the first two equations of Eq. (52) are independent from the last one. This allows the first two solutions of Eq. (52) being related as

$$\Phi_{12} = \Phi_{11} t_{go}, \tag{53}$$

and thus reduce the number of equations needed to be solved in Eq. (52) to three. For all three classical guidance laws, the expression for Z_{MT} has the same form and is given by

$$Z_{MT} = -\Phi_{11} V_r t_{go}^2 \dot{\lambda} + \boldsymbol{\Phi}_{1M} \boldsymbol{y}_M + \boldsymbol{\Phi}_{1T} \boldsymbol{y}_T. \tag{54}$$

The switching function given in Eq. (18), for arbitrary order dynamics, yields

$$s_{MT} = \Phi_{12}(d_T - d_M K_{u_T}) + \boldsymbol{\Phi}_{1M} k_M^{-1} \boldsymbol{B}_M K_{u_T} + \boldsymbol{\Phi}_{1T} k_T^{-1} \boldsymbol{B}_T. \tag{55}$$

Finally, for each classical guidance law $u_M^j \in \mathcal{U}_c$, an optimal (matched) evasion strategy u_T^{*j} of the form of Eq. (48) can be obtained using Eqs. (54) and (55), together with the corresponding solution $\boldsymbol{\Phi}_E^j$ to Eq. (52) matching the particular regime. It is important to note that s_{MT} is purely a function of t_{go}. Thus, more accurate t_{go} estimation yields to more precise timing of the required switches.

Remark 9. *The set of equations in Eq.* (52) *can be solved numerically, see [27] for more details. For special cases in which it is assumed that the target has ideal dynamics and the missile has first-order strictly proper dynamics, closed-form solutions have been derived in [12, 13] for PN and APN-guided missile with integer valued navigation constant N'.*

C. Target Evasion Based on Reduced-order MMAE

It is obvious that the reduced-order MMAE approach proposed in Sec. IVC cannot be used within the MMAC setting as the three regimes defined in Eq. (46) are functions of the unknown parameters N'_{PN}, N'_{APN}, and α. Thus, a matched (optimal) evasion u_T^{*j} against any $u_M^j \in \mathcal{U}_c^r$ can be only computed when the corresponding parameter (N'_{PN}, N'_{APN}, or α) has been identified. This leads to the following reduced-order evasion strategy:

$$u_T^{(red)} = \begin{cases} \varrho a_T^{max} & \text{if } \mu_k^j \neq 1,\ \forall j \in \{1 \dots p\} \ \text{ OR } \ t_{go} \geq 20 \times \tau_M^{max}, \\ \bar{\varrho} a_T^{max} \text{sign}(s_{MT}^j) & \text{otherwise,} \end{cases} \tag{56}$$

where s_{MT}^j is the switching function of Eq. (55) corresponding to the identified guidance law, i.e., PN, APN, or OGL, computed as in Sec. VB, using the respective estimated parameter N'_{PN}, N'_{APN}, or α, taken at time step when the "if" condition in Eq. (56) was first time violated. The design parameter ϱ can be chosen arbitrarily as ± 1 and defines the target's initial maneuver direction, τ_M^{max} stands for the largest time constant of the missile dynamics, and $\bar{\varrho}$ is defined as

$$\bar{\varrho} = \varrho \text{sign}(s_{MT}^j(t_{go} > 20 \times \tau_M^{max})) \tag{57}$$

to ensure that, if the guidance law j has been identified early enough, the resulting evasion strategy will follow the switches dictated entirely by s_{MT}^j. The condition $20 \times \tau_M^{max}$ is enforced in order to allow extra time to the estimation scheme to converge to the correct parameter N'_{PN}, N'_{APN}, or α. This is reasonable as the target switches occur at the very end of the engagement.

Note that any target maneuver direction switch (switches) occurring earlier than $\sim 20 \times \tau_M^{max}$ has a negligible effect on the resulting miss distance, but it might have a severe impact on the estimation performance, especially when bearing-only measurements are considered.

D. Implementation Issues

For practical implementation of the target's evasion strategy (as well as missile's guidance law), the time-to-go t_{go}, defined in Eq. (6), is commonly approximated as

$$\tilde{t}_{go} \approx -r/V_r, \qquad V_r < 0. \tag{58}$$

It has to be noted that observability in engagements with bearing-only measurements is a crucial factor in any guidance loop [19, 28]. If collision course conditions hold, i.e., the missile and target stay on the LOS, the range cannot be reconstructed from bearing-only measurements. A poor range estimation might result in inappropriate timing of the optimal switches dictated by s_{MT} and thus in a poor evasion performance. The only way how to improve $\tilde{t}_{go}$ accuracy is to improve range observability. Maneuvering away from the collision triangle, i.e., forcing the collision triangle to rotate, can improve the performance of the estimation process because, by altering the line of sight, the bearing measurement will return some insights on the relative range [19].

As outlined in Remark 4, $Z_{MT}(t)$ might cause chattering of u_T^*. This chattering might happen when $Z_{MT}(0) = 0$ and uncertain states are used to compute Z_{MT} (practical implementation). Such unwanted chattering of u_T (non-optimal bang-bang maneuvers) leads to a non-rotating collision triangle, thus poor range estimate and reduction of the achievable miss distance. A workaround to solve this problem is to use a dead-zone-like function applied on the sign of $Z_{MT}(t)$. By this, if

$$|Z_{MT}(t)| < \epsilon, \tag{59}$$

i.e., the ZEM distance is smaller than some prescribed value ϵ, the target will not change the direction of its maneuver command, unless the sign of $s_{MT}(t_{go})$ is changed or $|Z_{MT}(t)| \geq \epsilon$. Note that in the linear setting, $|Z_{MT}(t)|$ is a monotonically increasing function of time, see Eq. (24). Thus, by letting $\epsilon \to \infty$, it is actually assumed that the monotonically increasing property also holds for the nonlinear engagement. In that case, the nonlinear evasion strategy of Eq. (26) reduces to

$$u_T^* \approx a_T^{max} \text{sign}(s_{MT}) \text{sign}(Z_{MT}(0)), \qquad Z_{MT}(0) \neq 0. \tag{60}$$

If $Z_{MT}(0) = 0$, the evasion strategy for $u_T^*(0)$ can be chosen arbitrarily as either u_T^{max} or $-u_T^{max}$, and $\text{sign}(Z_{MT}(0)) \triangleq \text{sign}(u_T^*(0))$ should be assumed fixed in Eq. (60) throughout the engagement.

Let us now consider the above discussions within the MMAC configuration. Each "controller" in the bank has its own switching function s_{MT}^j entirely defined by $\mathbf{\Phi}_E^j$, pre-computed off-line using the u_M^j being correct assumption. Each s_{MT}^j is evaluated based on its own t_{go} estimate, which is calculated using Eq. (58) and $\hat{\boldsymbol{x}}_{k|k}^j$. To avoid chattering when $Z_{MT}^j(0) \approx 0$ for all $j \in \{1, \ldots, p\}$ (this can happen when all the filters in the bank are initialized with the same initial guess. Then, after the first measurement update, $Z_{MT}^j(0) = Z_{MT}^i(0), \forall i, j \in \{1, \ldots, p\}$ since $\boldsymbol{z}_0$ is the same for all filters), u_T^{*j} should be initialized with the same value (u_T^{max} or $-u_T^{max}$) for all j. By this, u_T computed using MMSE or MAP approach will not be affected by the initial transitions (convergence) of the probabilities μ_k^j. The probabilities will not play any role until the first switch occurs in any s_{MT}^j. Overall, this implementation ensures that the resulting target command u_T, computed by Eq. (47) or Eq. (49), will have a bang-bang structure and also it ensures that, in order to enhance observability, the best option is to maneuver away from the collision triangle.

The reduced-order approach, given in Sec. VC, is designed such that it is not affected by initial chattering. However the estimation problem is more challenging as there is an additional uncertainty on the guidance parameters, i.e., on N'_{PN}, N'_{APN}, and α, respectively. Therefore, one must ensure that the estimated guidance parameters, along with the estimated state and t_{go} approximation, have reasonable accuracy. A way to reduce noise in the guidance parameters is to apply a moving average on them.

VI. Performance Analysis

In this section, the set of "classical" missile guidance laws, presented in Sec. IVB, is used to demonstrate the performance of the proposed evasion concepts throughout numerical simulations. First, the simulation environment together with the interception scenario are presented, followed by a sample run analysis. Then, using Monte Carlo (MC) simulations, the estimation performance is analyzed in open loop and the miss distance is evaluated in closed loop.

A. Simulation Environment and Scenario

The planar nonlinear kinematics, missile and target dynamics, presented in Sec. A, are used for analysis. All engagements are initiated at a horizontal separation of 5 km between the missile and the target, thus $r_0 = 5000$ m and $\lambda_0 = 0$ rad. Both missile and target have constant speed. The target's speed is $V_T = 300$

m/s and the missile's speed is $V_M = 600$ m/s. For the analysis, it is assumed that the missile and the target have first-order strictly proper dynamics with time constants $\tau_M = 0.2$ s and $\tau_T = 0.5$ s. Hence, matrices in Eq. (7) degenerate to $\boldsymbol{A}_i = -1/\tau_i$, $\boldsymbol{B}_i = 1/\tau_i$, $\boldsymbol{C}_i = 1$, and $d_i = 0$, $i \in \{M, T\}$. The target's maneuver capability is limited to $a_T^{max} = 10$ g. No saturation is applied on the missile acceleration command u_M.

The EOM of the missile-target engagement are solved using a fourth-order Runge-Kutta (4RK) algorithm. The stopping criterion for the simulation is when V_r changes its sign (i.e., when $V_r \geq 0$). To ensure precise miss distance evaluation, high resolution integration is performed when the range is at range less than $r < 25\Delta t(V_M + V_T)$, where $\Delta t > 0$ is the nominal integration step. All studied engagements start with the missile and the target on a perfect collision triangle. Given the target's initial flight path angle γ_{T0}, the missile's initial flight path angle γ_{M0} is determined such that the initial collision conditions hold, i.e.,

$$V_M \sin(\gamma_{M0} - \lambda_0) - V_T \sin(\gamma_{T0} + \lambda_0) = 0. \tag{61}$$

The missile is assumed to have perfect information on the relative state, its own and target's parameters, respectively, and being guided towards the target using one of the following guidance laws: PN, APN or OGL, with navigation gains $\bar{\boldsymbol{N}}_i' \in \{3, 3.5, 4, 4.5, 5\}$ for $i = \{\text{PN}, \text{APN}\}$ and weights $\bar{\boldsymbol{\alpha}} \in \{0.0001, 0.001\}$ for OGL. The MMAE regimes of Eq. (45) are matched exactly to the above missile guidance laws and parameters, i.e., the navigation gains of PN and APN are represented by five regimes each, whereas for OGL two regimes are considered. Thus, in total, $p = 12$ EKFs are required to be run in parallel. In the case of the reduced-order MMAE, only $p = 3$ filters are designed and run, matching the above guidance laws of PN, APN and OGL, however without good knowledge about the respective guidance parameters. The prior probability of each guidance law is 1/3 and the initial probability of each regime is equal within the respective guidance law, i.e., $\mu_0^i = 1/15$, $i = 1, \ldots, 10$ and $\mu_0^{11} = \mu_0^{12} = 1/6$.

The estimation problem formulated in Sec. IV address two possible sensor choice combinations, see Sec. IIC. However, in our simulations, only the more difficult case is considered in which the target has bearing-only measurements. The states needed for the proposed evasion strategy employment are estimated at a frequency of 200 Hz (i.e., $T_s = 1/200$ s). The nonlinear EOM of Eq. (32) are propagated using the 4RK algorithm. The measurements are acquired at a sampling frequency of 50 Hz (i.e., $T_s^m = 1/50$ s). The simulated measurement noises are with $\sigma_\lambda = 1$ mrad. The tuning parameters of the EKFs have been chosen by numerical simulations. A blind range of 50 m is assumed. If $r < 50$, no new measurements are acquired and the EKFs work in open loop, i.e., perform only the time propagation step at a given rate T_s. All filters in the bank are initialized with the same initial conditions sampled from a Gaussian distribution, i.e., $\hat{\boldsymbol{x}}_{0|0} \sim \mathcal{N}(\boldsymbol{x}_0, \boldsymbol{P}_{0|0})$, where $\boldsymbol{x}_0$ is the true state vector and $\boldsymbol{P}_{0|0} = \text{diag}\left(50^2, (3\pi/180)^2, (1\text{g})^2, (3\pi/180)^2, 50^2\right)$ is the initial covariance matrix of the filters. For the reduced-order MMSE approach, the covariance matrix $\boldsymbol{P}_{0|0}$ is augmented for each EKF with an additional diagonal element of the value of 5^2, 5^2, and 0.008^2, corresponding to the uncertainty on the guidance parameter N'_{PN}, N'_{APN}, and α, respectively. After the filters are initialized, they run recursively on their own estimates. Their likelihood functions are used to update the mode probabilities. The latest mode probabilities are used to compute the target evasion evasion command.

B. Sample Run

A sample run of a target evasion from a PN-guided missile with $N'_{PN} = 4$ is considered here. The considered initial flight path angle of the target is $\gamma_{T0} = \pi/12$ rad. The initial flight path angle of the missile γ_{M0} satisfies Eq. (61).

Figure 3 shows the planar trajectories of the missile and target in the simulated sample run. Particularly, the target assumes perfect information, i.e., uses true states and its evasion strategy is exactly matched to the active missile guidance law and parameters. Also, the time-to-go required by the evasion law is computed as in Eq. (58), where range and range-rate are obtained from the true relative position and relative velocity. The resulting miss distance in this sample scenario is approximately 0.51 m. It can be seen that the applied evasion strategy also forces the collision triangle to rotate with time.

Based on the same sample run, Figs. 4-5 present, among others, the posterior probabilities $\bar{\boldsymbol{\mu}}_k = [\mu_k^{PN}, \mu_k^{APN}, \mu_k^{OGL}]$ of each guidance law being correct as a function of time for different MMAE approaches. Figure 4 shows the behavior of $\bar{\boldsymbol{\mu}}_k$ and the probability μ_k^j, $j = 1, \ldots, 12$ of each guidance law parameter (regime) being correct for the full-order MMAE approach. In this case, the PN guidance law has been identified as the missile's guidance law in approximately 1 sec, and after approximately 2.5 sec its navigation gain has also been correctly identified.

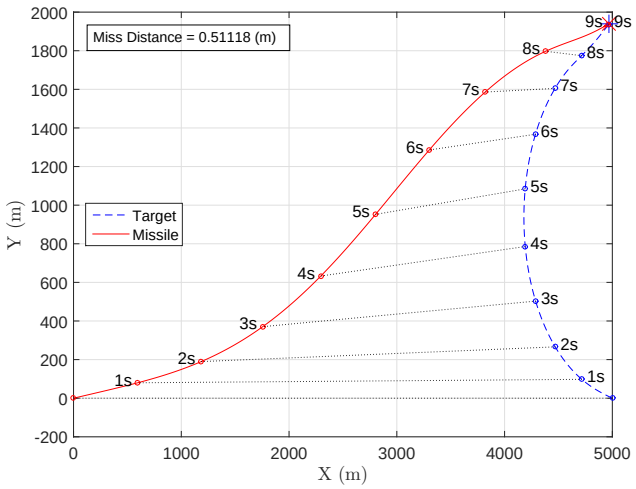

Figure 3: Planar engagement trajectories of a missile-target engagement. Missile uses PN with $N'_{PN} = 4$. Target MMAC with MMSE.

Figure 5 depicts the posterior probabilities $\bar{\boldsymbol{\mu}}_k$ of each guidance law being correct and the estimated guidance parameters, N'_{PN}, N'_{APN}, and α, using the reduced-order MMAE. It can be seen that the correct guidance law takes a bit longer to be identified in this sample run, i.e., approximately 2 sec. However, the correct guidance parameter $N'_{PN} = 4$ is identified after approximately 3 sec. A 1 sec moving average window is used to mitigate the impact of the noise estimate. Note that as soon as the probability of a particular filter reaches 0, it is turned off, thus allowing additional computational savings.

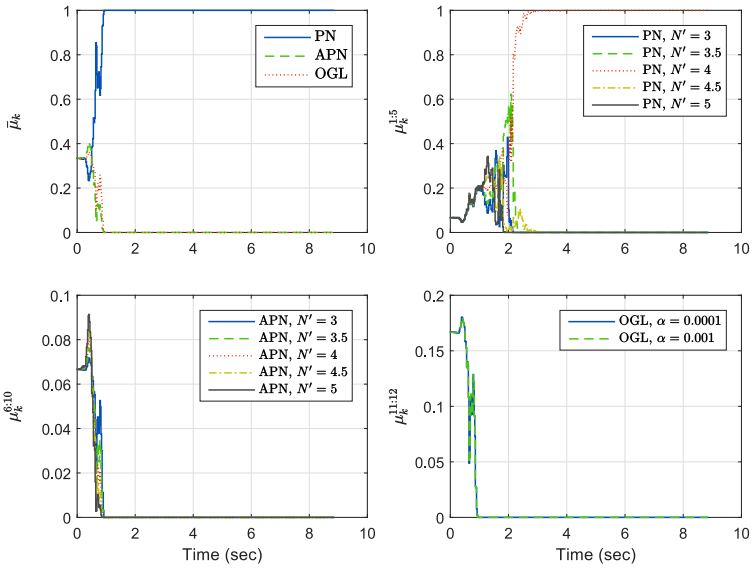

Figure 4: Full-order MMAE approach's sample regime probabilities. Missile uses PN with $N'_{PN} = 4$.

Figure 6 presents the acceleration profiles of the target for different scenarios. In this figure, the acceleration a_T (solid line) is driven by the target's acceleration command u_T (dashed line). The top frame shows the optimal sequence and timing of the target switches against a missile employing PN guidance law with $N'_{PN} = 4$. This evasion is obtained when the target assumes perfect information. The other three frames below represent the proposed MMAE-based approaches: MMAC with MMSE, MMAC with MAP, and the reduced-order approach of Sec. VC. It can be seen that while both MMAC approaches perform almost identically to the perfect information (optimal) case, the reduced-order approach executes the first switch with some chattering. This occurs, as will be shown in the next subsection, due to less accurate

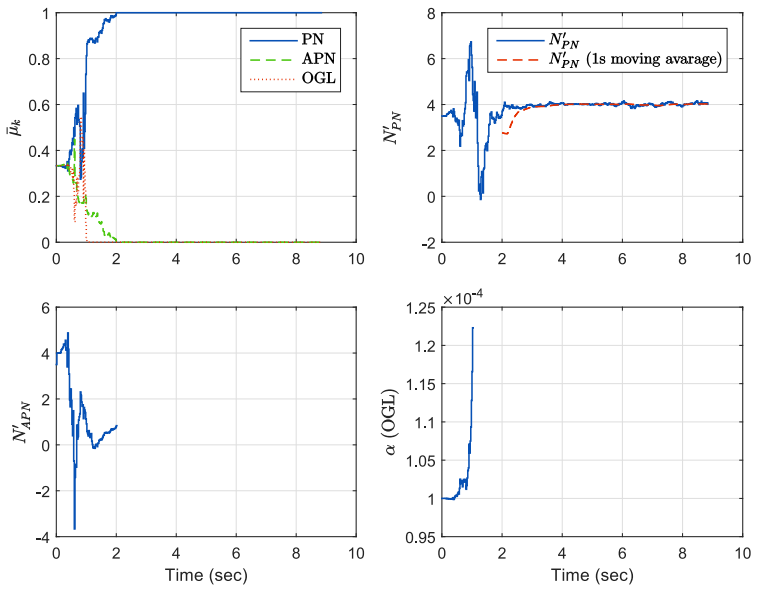

Figure 5: Reduced-order MMAE approach's sample regime probabilities and guidance parameter estimates. Missile uses PN with $N'_{PN} = 4$.

time-to-go estimation. It can be also noticed that the optimal switches occur approximately 1.5 sec before the end of the engagement ($t_{go} \approx 1.5$). This confirms the proposed bound $20 \times \tau_M = 4$ sec in Eq. (56) for the reduced-order approach.

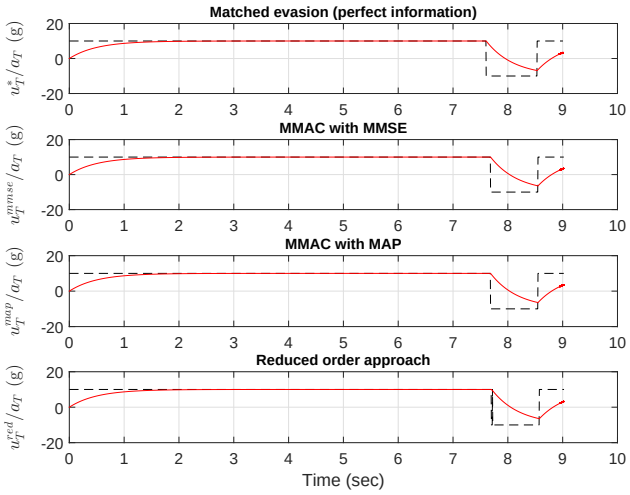

Figure 6: Target acceleration and acceleration command for different scenarios. Target evasion against n PN guided missile with $N'_{PN} = 4$.

C. Monte Carlo Study - Open Loop

To demonstrate and compare the estimation performance of the full-order and the reduced-order MMAE approach, a 500-run MC simulation campaign was performed considering bearing-only measurements. To allow a fair comparison between the two approaches, perfect information is used again to compute the optimal target evasion strategy. This allows to consider, in each MC run, the same measurement and target controls sequences for both MMAE approaches. However, in each MC run, the filters are initiated with different random initial guess, see Sec. VI.A, and different noise seeds are used to generate the measurement noises. The same engagement scenario is considered here as in the previous subsection, i.e., the missile uses PN

guidance with $N'_{PN} = 4$. The target's initial angle is $\gamma_{T0} = \pi/12$.

Figures 7-11 present the obtained state estimation results for both approaches. The errors shown are computed using the blended state estimates, $\hat{\boldsymbol{x}}_{k|k}$, and blended covariances, $\boldsymbol{P}_{k|k}$, computed using the mode-conditioned state estimates $\hat{\boldsymbol{x}}^j_{k|k}$ and error covariances $\boldsymbol{P}^j_{k|k}$ as follows

$$\hat{\boldsymbol{x}}_{k|k} = \sum_{i=1}^{p} \mu^j_k \hat{\boldsymbol{x}}^j_{k|k},$$

$$\boldsymbol{P}_{k|k} = \sum_{i=1}^{p} \mu^j_k \left(\boldsymbol{P}^j_{k|k} + (\hat{\boldsymbol{x}}^j_{k|k} - \hat{\boldsymbol{x}}_{k|k})(\hat{\boldsymbol{x}}^j_{k|k} - \hat{\boldsymbol{x}}_{k|k})^T \right).$$

Additionally to the estimated states, the time-to-go approximation errors (function of the estimated states) are also shown in Fig. 12. In all the figures, the dash-dotted line stands for the mean of the estimation errors, the solid line is the error from a sample run, the thick solid line is the actual standard deviation (actual 1σ) of the estimation errors, the dotted line is the sample run's 1σ estimation error bound ($\pm\sigma_{filter}$) predicted by the filter, and the vertical dashed line indicates the beginning of the blind range of the sensor. Note that the sample run (sample error and $\pm\sigma_{filter}$) shown in Figs. 7-12 corresponds to the same sample run as presented in the previous "Sample Run" subsection in Figs. 4-5.

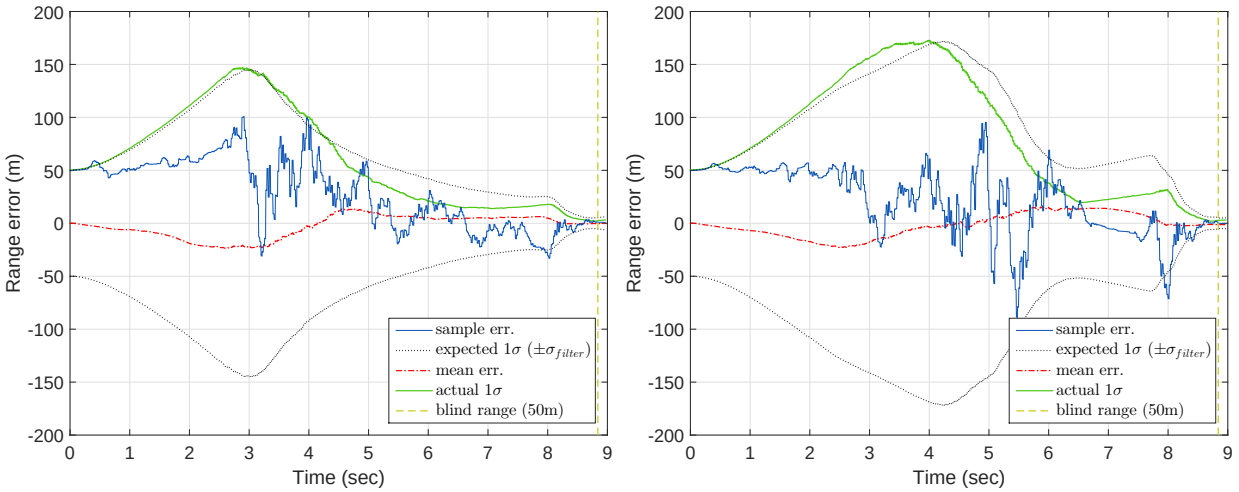

(a) Full-order MMAE with 12 regimes

(b) Reduced-order MMAE with 3 regimes

Figure 7: Range estimation error performance

The obtained results show relatively fast convergence of all of the estimated states but the range. Especially note the small error in estimating the missile's acceleration, which is in general known to be hard to estimate. The hangoff errors that can be seen in most of the cases at the beginning of the engagement are due to the initial transitions (convergence) of the weights when the correct regime has still not been identified and some filters might be already diverging. However, when the filter is matched, i.e., the regime probabilities converged, the estimates becomes very good. It can be also observed that the standard deviations of the errors (actual 1σ) are consistent with those predicted by the filter. The results also suggest that the reduced-order approach has slightly worse estimation performance than the full-order approach. This is obvious since it deals with additional uncertainty on the missile guidance parameters.

Despite the poor range estimate, the time-to-go approximation yields relatively good performance, see Fig. 12. This is especially important as the time-to-go is primarily used in the proposed evasion concept and, as it was discussed earlier, its accuracy is considered to have significant effect on the closed loop evasion performance (resulting miss distance). This will be studied in the next subsection. It should be noted that measurements with $T^m_s = 1/25$ s and $\sigma_\lambda = 2$ mrad were also considered. The obtained results did not differ significantly from those presented in this section. Thus, we have omitted these results for brevity of the presentation.

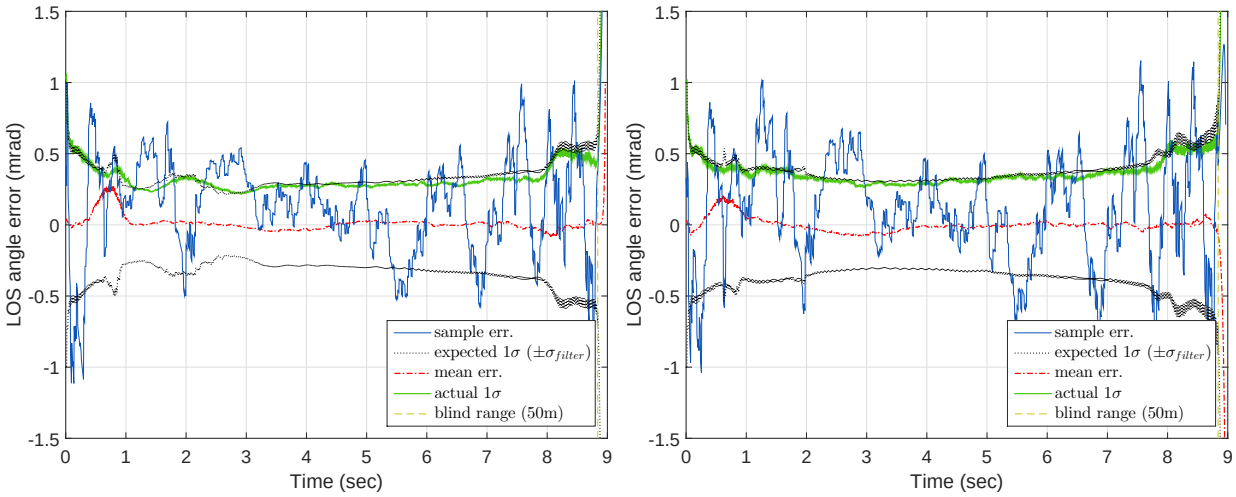

(a) Full-order MMAE with 12 regimes

(b) Reduced-order MMAE with 3 regimes

Figure 8: LOS angle estimation error performance

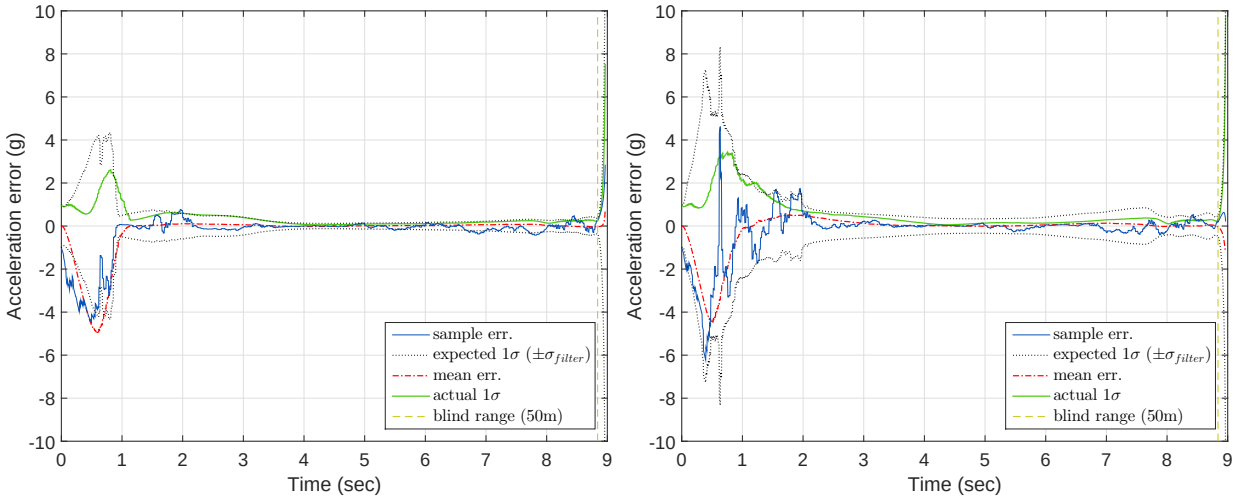

(a) Full-order MMAE with 12 regimes

(b) Reduced-order MMAE with 3 regimes

Figure 9: Missile acceleration estimation error performance.

D. Monte Carlo Study - Closed Loop

Here, the effect of the "estimator in the loop" on the closed-loop performance of the proposed evasion strategies is evaluated and compared with: *i*) the case when the target performs optimal evasion matched to the missile's active guidance strategy (perfect information case), and *ii*) the case when the target, throughout the entire engagement, applies maximal acceleration command to one side (blind evasion).

The analysis is based on a set of 500 MC runs. The performance is compared in terms of the achieved miss distance. All engagements start with the missile and the target being on the collision triangle. For each run, the active missile guidance strategy, u_M^j, was randomly selected among the 12 possible regimes, presented in Sec. VI.A, and obeying its initial probability μ_0^j. The considered engagement scenario is symmetric with respect to the X-axis. Thus, only positive values of γ_{T0} are considered. These values are uniformly drawn from the interval $[0, \pi/6]$ rad.

Figure 13 presents the obtained miss distances by means of the cumulative distribution functions (CDFs). The expected miss distance Miss_{exp}, defined in Sec. III.B, is also considered for illustration. The results suggest that the achieved evasion performances of the two full-order approaches, i.e., MMAC with MMSE

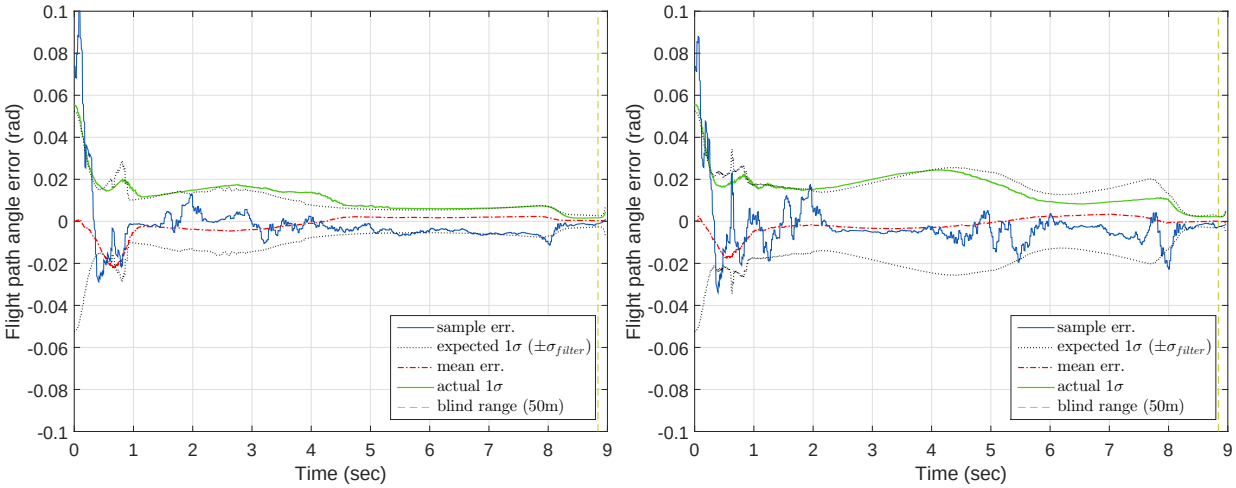

(a) Full-order MMAE with 12 regimes

(b) Reduced-order MMAE with 3 regimes

Figure 10: Missile flight path angle estimation error performance

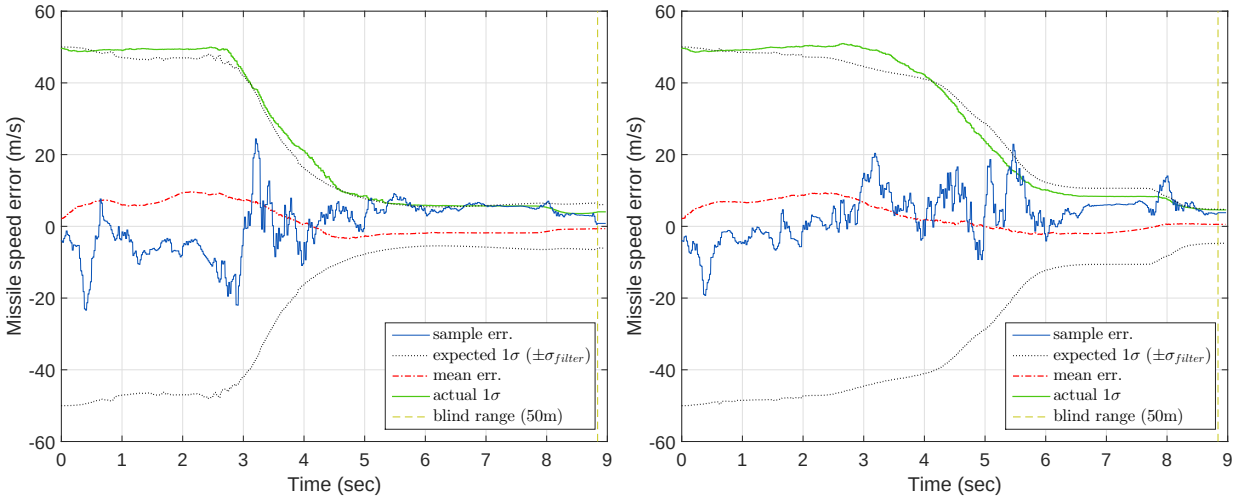

(a) Full-order MMAE with 12 regimes

(b) Reduced-order MMAE with 3 regimes

Figure 11: Missile velocity estimation error performance

and MMAC with MAP, are relatively close to the evasion performance of the deterministic scenario when the target has perfect information. It can be also seen that MMSE and MAP blending yield very similar performance. The evasion performance slightly deteriorates when the reduced-order approach is considered. However, it still performs much better than the blind evasion to one side. Note that the above presented results correspond to bearing-only measurements. It is obvious that the evasion performance could be further improved by using an additional measurement of the relative range, yielding to more accurate time-to-go estimate.

VII. Conclusion

Multiple model adaptive evasion strategies for a target aircraft from a homing missile employing a linear guidance law have been proposed. The performance of these schemes has been analyzed through extensive Monte Carlo simulations. It was shown that the proposed approaches allow fast enough identification of the employed missile guidance strategy and thus enabling the target to apply, early enough, the optimal

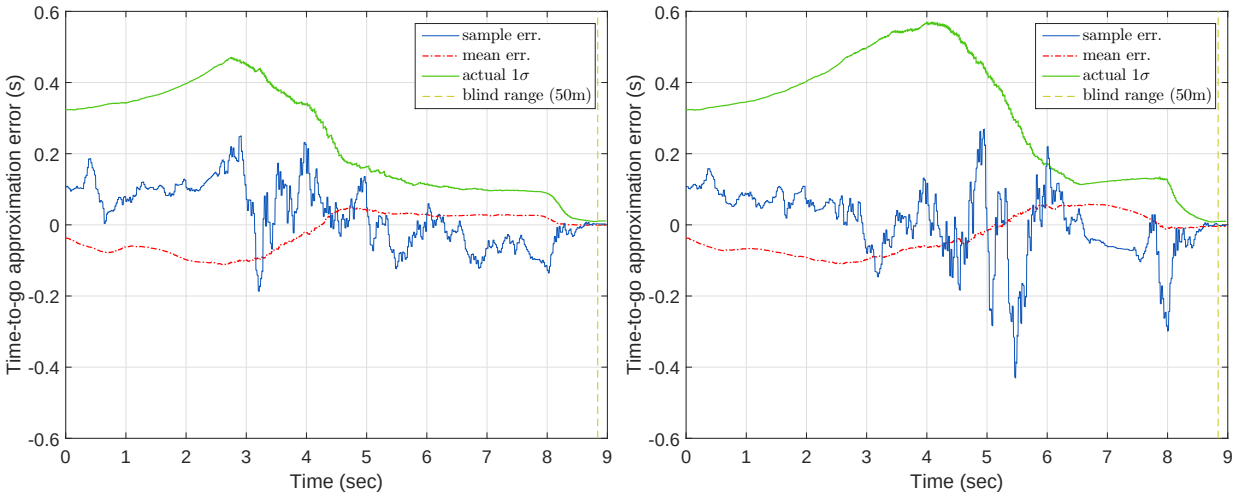

(a) Full-order MMAE with 12 regimes

(b) Reduced-order MMAE with 3 regimes

Figure 12: Time-to-go approximation error performance

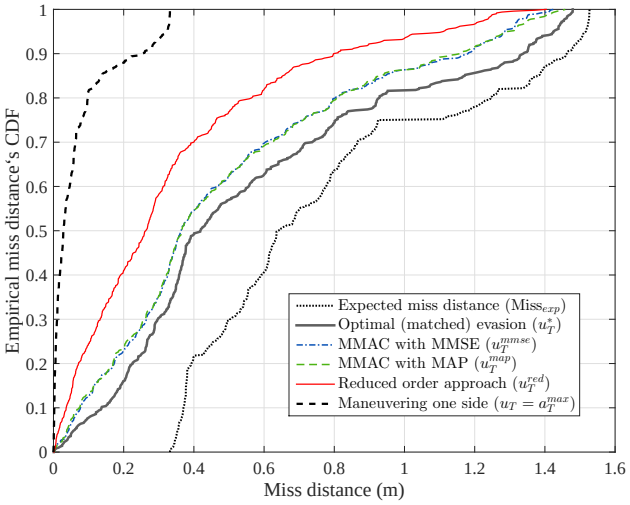

Figure 13: Miss distance CDF based on 500 Monte Carlo runs.

evasion maneuvers matched to the missile's active guidance. Moreover, the proposed evasion methods force the collision triangle to rotate, thus helping to enhance observability, especially that of the range which is critical when the target aircraft acquires LOS angle measurements only. From evasion perspective, for the missile and target having first-order linear dynamics, it was shown that the resulting evasion performance, achieved by the full-order approach (imperfect information), is very close to the best performance achievable (perfect information). This comparison thus indicates that, for targets having limited maneuver capability and carrying sensors that provide bearing-only measurements, the degradation in avoidance capability from a homing missile may not be as serious as it could have been expected.

Acknowledgments

This effort was sponsored by the U.S. Air Force Office of Scientific Research, Air Force Materiel Command, under grant number FA9550-15-1-0429. The U.S. Government is authorized to reproduce and distribute reprints for Governmental purpose notwithstanding any copyright notation thereon.

References

[1] Zarchan, P., *Tactical and Strategic Missile Guidance*, Vol. 199 of *Progress in Astronautics and Aeronautics*, AIAA, Reston, VA, 4th ed., 2002. Chap. 2.

[2] Yuan, L. C., "Homing and Navigational Courses of Automatic Target Seeking Devices," *Journal of Applied Physics*, Vol. 19, No. 12, 1948, pp. 1122–1128, doi:10.1063/1.1715028.

[3] Garber, V., "Optimum Intercept Laws for Accelerating Targets," *AIAA Journal*, Vol. 6, No. 11, 1968, pp. 2196–2198, doi:10.2514/3.4962.

[4] Cottrell, R. G., "Optimal Intercept Guidance for Short-Range Tactical Missiles," *AIAA journal*, Vol. 9, No. 7, 1971, pp. 1414–1415, doi:10.2514/3.6369.

[5] Asher, R. and Matuszewski, J. P., "Optimal Guidance with Maneuvering Targets," *Journal of Spacecraft and Rockets*, Vol. 11, No. 3, 1974, pp. 204–206, doi:10.2514/3.62041.

[6] Speyer, J. L., "An adaptive terminal guidance scheme based on an exponential cost criterion with application to homing missile guidance," *IEEE Transactions on Automatic Control*, Vol. 21, No. 3, 1976, pp. 371–375, doi:10.1109/TAC.1976.1101206.

[7] Fitzgerald, R. and Zarchan, P., "Shaping filters for randomly initiated target maneuvers," in "Proceedings of AIAA Guidance and Control Conference," AIAA, New York, Aug. 1978, pp. 424–430. Also AIAA Paper 1978-1304, 1987.

[8] Besner, E. and Shinar, J., "Optimal Evasive Maneuvers in Conditions of Uncertainty," Tech. rep., Technion - IIT, 1979.

[9] Zarchan, P., "Proportional navigation and weaving targets," *Journal of Guidance, Control, and Dynamics*, Vol. 18, No. 5, 1995, pp. 969–974, doi:10.2514/3.21492.

[10] Forte, I., Steinberg, A., and Shinar, J., "The effects of non-linear kinematics in optimal evasion," *Optimal Control Applications and Methods*, Vol. 4, No. 2, 1983, pp. 139–152, doi:10.1002/oca.4660040204.

[11] Borg, D. and Julich, P., "Proportional navigation vs an optimally evading, constant-speed target in two dimensions," *Journal of Spacecraft and Rockets*, Vol. 7, No. 12, 1970, pp. 1454–1457, doi:10.2514/3.30190.

[12] Shinar, J. and Steinberg, D., "Analysis of optimal evasive maneuvers based on a linearized two-dimensional kinematic model," *AIAA Journal of Aircraft*, Vol. 14, No. 8, 1977, pp. 795–802, doi:10.2514/3.58855.

[13] Shima, T., "Optimal cooperative pursuit and evasion strategies against a homing missile," *Journal of Guidance, Control, and Dynamics*, Vol. 34, No. 2, 2011, pp. 414–425, doi:10.2514/1.51765.

[14] Shaferman, V. and Shima, T., "Cooperative multiple-model adaptive guidance for an aircraft defending missile," *Journal of guidance, control, and dynamics*, Vol. 33, No. 6, 2010, pp. 1801–1813, doi:10.2514/1.49515.

[15] Speyer, J. L., Hull, D. G., Larson, S., and Tseng, C., "Estimation enhancement by trajectory modulation for homing missiles," *Journal of Guidance, Control, and Dynamics*, Vol. 7, No. 2, 1984, pp. 167–174, doi:10.2514/3.8563.

[16] Farina, A., "Target tracking with bearings–only measurements," *Signal processing*, Vol. 78, No. 1, 1999, pp. 61–78, doi:10.1016/S0165-1684(99)00047-X.

[17] Song, T. L. and Um, T. Y., "Practical guidance for homing missiles with bearings-only measurements," *IEEE Transactions on Aerospace and Electronic Systems*, Vol. 32, No. 1, 1996, pp. 434–443, doi:10.1109/7.481284.

[18] Shaferman, V. and Oshman, Y., "Cooperative interception in a multi-missile engagement," in "AIAA Guidance, Navigation, and Control Conference and Exhibit," Chicago, IL, Aug. 2009, doi:10.2514/6.2009-5783. AIAA Paper 2009-5783.

[19] Battistini, S. and Shima, T., "Differential games missile guidance with bearings-only measurements," *IEEE Transactions on Aerospace and Electronic Systems*, Vol. 50, No. 4, 2014, pp. 2906–2915, doi:10.1109/TAES.2014.130366.

[20] Magill, D. T., "Optimal adaptive estimation of sampled stochastic processes," *IEEE Transactions on Automatic Control*, Vol. 10, No. 4, 1965, pp. 434–439, doi:10.1109/TAC.1965.1098191.

[21] Bar-Shalom, Y., Li, X. R., and Kirubarajan, T., *Estimation with applications to tracking and navigation: theory algorithms and software*, John Wiley & Sons, Inc., New York, NY, 2001. Chap. 11.

[22] Arulampalam, M. S., Maskell, S., Gordon, N., and Clapp, T., "A tutorial on particle filters for online nonlinear/non-Gaussian Bayesian tracking," *IEEE Transactions on Signal Processing*, Vol. 50, No. 2, 2002, pp. 174–188, doi:10.1109/78.978374.

[23] Julier, S. J. and Uhlmann, J. K., "Unscented filtering and nonlinear estimation," *Proceedings of the IEEE*, Vol. 92, No. 3, 2004, pp. 401–422, doi:10.1109/JPROC.2003.823141.

[24] Perelman, A., Shima, T., and Rusnak, I., "Cooperative differential games strategies for active aircraft protection from a homing missile," *Journal of Guidance, Control, and Dynamics*, Vol. 34, No. 3, 2011, pp. 761–773, doi:10.2514/1.51611.

[25] Lainiotis, D. G., "Partitioning: A unifying framework for adaptive systems, II: Control," *Proceedings of the IEEE*, Vol. 64, No. 8, 1976, pp. 1182–1198, doi:10.1109/PROC.1976.10289.

[26] Athans, M., Castanon, D., Dunn, K. P., Greene, C. S., Lee, W. H., Sandell, N. R., and Willsky, A. S., "The stochastic control of the F-8C aircraft using a multiple model adaptive control (MMAC) method–Part I: Equilibrium flight," *IEEE Transactions on Automatic Control*, Vol. 22, No. 5, 1977, pp. 768–780, doi:10.1109/TAC.1977.1101599.

[27] Gutman, S., *Applied min-max approach to missile guidance and control*, Vol. 209 of *Progress in Astronautics and Aeronautics*, AIAA, Reston, VA, 2005. Chap. 9.

[28] Hepner, S. A. and Geering, H. P., "Observability analysis for target maneuver estimation via bearing-only and bearing-rate-only measurements," *Journal of Guidance, Control, and Dynamics*, Vol. 13, No. 6, 1990, pp. 977–983, doi:10.2514/3.20569.